Learning scale-variant and scale-invariant features for deep image classification

Nanne van Noord and Eric Postma
Tilburg center for Communication and Cognition, School of Humanities
Tilburg University, The Netherlands
Email: {n.j.e.vannoord, e.o.postma}@tilburguniversity.edu

Abstract—**Convolutional Neural Networks (CNNs) require large image corpora to be trained on classification tasks. The variation in image resolutions, sizes of objects and patterns depicted, and image scales, hampers CNN training and performance, because the task-relevant information varies over spatial scales. Previous work attempting to deal with such scale variations focused on encouraging scale-invariant CNN representations. However, scale-invariant representations are incomplete representations of images, because images contain scale-variant information as well. This paper addresses the combined development of scale-invariant and scale-variant representations. We propose a multi-scale CNN method to encourage the recognition of both types of features and evaluate it on a challenging image classification task involving task-relevant characteristics at multiple scales. The results show that our multi-scale CNN outperforms single-scale CNN. This leads to the conclusion that encouraging the combined development of a scale-invariant and scale-variant representation in CNNs is beneficial to image recognition performance.**

I. INTRODUCTION

Convolutional Neural Networks (CNN) have drastically changed the computer vision landscape by considerably improving the performance on most image benchmarks [1], [2]. A key characteristic of CNNs is that the deep(-based) representation, used to perform the classification, is generated from the data, rather than being engineered. The deep representation determines the type of visual features that are used for classification. In the initial layers of the CNN, the visual features correspond to oriented edges or color transitions. In higher layers, the visual features are typically more complex (e.g., conjunctions of edges or shapes). Finding the appropriate representation for the task at hand requires presenting the CNN with many instances of a visual entity (object or pattern) in all its natural variations, so that the deep representation captures most naturally occurring appearances of the entity.

Three main sources of natural variation are the location, the viewpoint, and the size of an object or pattern. Variations in location are dealt with very well by a CNN [3], which follows naturally from the weight sharing employed in the convolution layers [4]. CNNs can also handle variations in viewpoint by creating filters that respond to viewpoint-invariant features [5]. Size variations pose a particular challenge in CNNs [6], especially when dealing with image corpora containing images of varying resolutions and depicting objects and patterns at different sizes and scales, as a result of varying distances from the camera and blurring by optical imperfections, respectively. This leads to variations in image resolution, object size, and

image scale, which are two different properties of images. The relations between image resolution, object size, and image scale is formalized in digital image analysis using Fourier theory [7]. Spatial frequencies are a central concept in the Fourier approach to image processing. Spatial frequencies are the two-dimensional analog of frequencies in signal processing. The fine details of an image are captured by high spatial frequencies, whereas the coarse visual structures are captured by low spatial frequencies. In what follows, we provide a brief intuitive discussion of the relation between resolution and scale, without resorting to mathematical formulations.

A. Image resolution, object size, and image scale

Given an image its resolution can be expressed in terms of the number of pixels (i.e., the number of samples taken from the visual source); low resolution images have fewer pixels than high resolution images. The scale of an image refers to its spatial frequency content. Fine scale images contain the range from high spatial frequencies (associated with small visual structures) down to low spatial frequencies (with large visual structures). Coarse scale images contain low spatial frequencies only. The operation of spatial smoothing (or blurring) of an image corresponds to the operation of a low-pass filter: high spatial frequencies are removed and low spatial frequencies are retained. So, spatial smoothing a fine scale image yields a coarser scale image.

The relation between the resolution and the scale of an image follows from the observation that in order to represent visual details, an image should have a resolution that is sufficiently high to accommodate the representation of the details. For instance, we consider the chessboard pattern shown in Figure 1a. Figure 1b shows a 6×6 pixel reproduction of the chessboard pattern. The resolution of the reproduction is insufficient to represent the fine structure of the chessboard pattern. The distortion of an original image due to insufficient resolution (or sampling) is called *aliasing* [7].

As this example illustrates, image resolution imposes a limit to the scale at which visual structure can be represented. Figure 1c displays the space spanned by resolution (horizontal axis) and scale (vertical axis). The limit is represented by separation of the shaded and unshaded regions. Any image combining a scale and resolution in the shaded area suffers from aliasing. The sharpest images are located at the shaded-

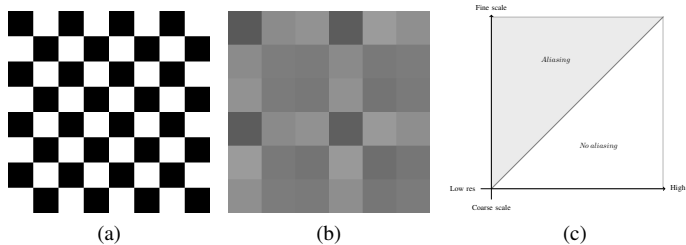Fig. 2.   Artwork *'Hoefsmid bij een ezel'* by Jan de Visscher.

Fig. 1.   Illustration of aliasing. (a) Image of a chessboard. (b) Reproductions of the chessboard with an image of insufficient resolution (6 × 6 pixels). The reproduction is obtained by applying bicubic interpolation. (c) The space spanned by image resolution and image scale. Images defined by resolution-scale combinations in the shaded area suffer from aliasing. See text for details.

unshaded boundary. Blurring an image corresponds to a vertical downward movement into the unshaded region

Having discussed the relation between resolution and scale, we now turn to the discussion of the relation of object size to resolution and scale. Real-world images with a given scale and resolution contain objects and structures at a range of sizes [8], For example, the image of the artwork shown in Figure 2, depicts large-sized objects (people and animals) and small-sized objects (hairs and branches). In addition, it may contain visual texture associated with the paper it was printed on and with the tools that were used used to create the artwork. Importantly, the same object may appear at different sizes. For instance, in the artwork shown there persons depicted at different sizes. The three persons in the middle are much larger in size than the one at the lower right corner. The relation between image resolution and object size is that the resolution puts a lower bound on the size of objects that can be represented in the image. If the resolution is too low, the smaller objects cannot be distinguished anymore. Similarly,

the relation between image scale and object size is that if the scale becomes too coarse, the smaller objects cannot be distinguished anymore. Image smoothing removes the high-spatial frequencies associated with the visual characteristics of small objects.

B. Scale-variant and scale-invariant image representations

Training CNNs on large image collections that often exhibit variations in image resolution, depicted object sizes, and image scale, is a challenge. The convolutional filters, which are automatically tuned during the CNN training procedure, have to deal with these variations. Supported by the acquired filters the CNN should ignore task-irrelevant variations in image resolution, object size, and image scale and take into account task-relevant features at a specific scale. The filters providing such support are referred to as scale-invariant and scale-variant filters, respectively [9].

The importance of scale-variance was previously highlighted by Gluckman [9] and Park et al. [10], albeit for two different reasons. The first reason put forward by Gluckman arises from the observation that images are only partially described by scale invariance [9]. When decomposing an image into its scale-invariant components, by means of a scale-invariant pyramid, and subsequently reconstructing the image based on the scale-invariant components the result does not fully match the initial image, and the statistics of the resulting image do not match those of natural images. For training a CNN this means that when forcing the filters to be scale-invariant we might miss image structure which is relevant to the task. Gluckman demonstrated this, by means of his proposed space-variant image pyramids, which separate scale-specific from scale-invariant information in [9] and found that object recognition benefited from scale-variant information.

The second reason was presented by Park et al. in [10], where they argue that the need for scale-variance emerges from the limit imposed by image resolution, stating that "Recognizing a 3-pixel tall object is fundamentally harder than recognizing a 300-pixel object or a 3000-pixel object." [10, p. 2]. While recognising very large objects comes with it own challenges, it is obvious that the recognition task can be very different depending on the resolution of the image. Moreover, the observation that recognition changes based on the resolution ties in with the previously observed interaction between resolution and scale: as a reduction in resolution also changes the scale. Park et al. identify that most multi-scale models ignore that most naturally occurring variation in scale, within images, occurs jointly with variation in resolution, i.e. objects further away from the camera are represented at a lower scale and at a lower resolution. As such they implement a multi-resolution model and demonstrate that explicitly incorporating scale-variance boosts performance.

Inspired by these earlier studies, we propose a multi-scale CNN which explicitly deals with variation in resolution, object size and image scale, by encouraging the development of filters which are scale-variant, whilst constructing a representation that is scale-invariant.

The remainder of this paper is organised as follows. Section II contains an overview of previous work that deals with scale variation for learning deep image representations. In Section III we provide a detailed presentation of our multi-scale CNN for scale-invariant and scale-variant filters. Section IV outlines the task used for evaluating the performance of the multi-scale CNN. In Section V the experimental setup is described, including the dataset and the experimental method. In Section VI the results of the experiments are presented. We discuss the implications of using multi-scale CNNs in Section VII. Finally, Section VIII concludes by stating that combining scale-variant and scale-invariant features contributes to image classification performance.

II. Previous work

In this paper, we examine learning deep image representations that incorporate scale-variant and/or scale-invariant visual features by means of CNNs. Scale variation in images and its impact on computer vision algorithms is a widely studied problem [8], [11], where invariance is often regarded as a key property of a representation [12]. It has been shown that under certain conditions CNN will develop scale-invariant filters [13]. Additionally, various authors have investigated explicitly incorporating scale-invariance in deep representations learnt by CNN [14], [6], [3], [15], [16]. While these approaches successfully deal with scale-invariance they forgo the problem of recognising scale-variant features at multiple scales [10].

Standard CNN trained without any data augmentation will develop representations which are scale-variant. As such it is only capable of recognising the features it was trained on, at the scale it was trained on, such a CNN cannot deal with scale-variant features at different scales. A straightforward solution to this limitation is to expose the CNN to multiple scales during training, this approach is typically referred to as scale jittering [17], [18], [19]. It is commonly used as a data augmentation approach to increase the amount of training dataset, and as a consequence reduce overfitting. Additionally, it has been shown that scale jittering improves classification performance [18]. While part of the improved performance is due to the increase in training data and reduced overfitting, scale jittering also allows the CNN to learn to recognise more scale-variant features, and potentially develop scale-invariant filters. Scale-invariant filters might emerge from the CNN being exposed to scale variants of the same feature. However, *standard* CNN typically do not develop scale-invariant filters [13], and instead will require more filters to deal with the scaled variants of the same feature [6], in addition to the filters needed to capture scale-variant features. A consequence of this increase in parameters, which increases further when more scale variation is introduced, is that the CNN becomes more prone to overfit and training the network becomes more difficult in general. In practice this limits scale-jittering to small scale variations. Moreover, scale-jittering is typically implemented as jittering the resolution, rather than explicitly changing the scale, which potentially means that jittered versions are actually of the same scale.

One approach that is able to deal with larger scale variations, whilst offering many of the same benefits as scale jittering is multi-scale training [20]. Multi-scale training consists of training separate CNN on fixed size crops of resized versions of the same image. At test time the softmax class posteriors of these CNN are averaged into a single prediction, taking advantage of the information from different scales and model averaging [21], resulting in improved performance over single scale classification. However, because the work by Wu et al. [20] is applied to datasets with a limited image resolution, they only explore the setting in which multi-scale training is applied for a relatively small variation in scales, and only two scales. Moreover, as dealing with scale variation is not an explicit aim of their work they do not analyse the impact of dealing with multiple scales, beyond that it increases their performance. Finally, because of the limited range of scales they explored they do not deal with aliasing due to resizing. Aliasing is harmful for any multi-scale approach as it produces visual artifacts which would not occur in natural images of the reduced scale, whilst potentially obfuscating relevant visual structure at that scale.

In this work we aim to explicitly learn scale-variant features for large variations in scale, and make the following three contributions: (1) We present a modified version of multi-scale training that explicitly creates multiple scales, reducing aliasing due to resizing, allowing us to compare larger scale differences whilst reducing redundancy between scales. (2) We introduce a novel dataset of high resolution images that allows us to explore the effects of larger scale variations. (3) We perform an in-depth analysis of the results and compare different scale combinations in order to increase our understanding of the influence of scale-variation on the classification performance.

III. MULTI-SCALE CONVOLUTIONAL NEURAL NETWORK

In this Section we present the multi-scale CNN by explaining how a standard (single-scale) CNN performs a spatial decomposition of images. Subsequently, we motivate the architecture of the multi-scale CNN in terms of the scale-dependency of the decomposition.

CNNs perform a stage-wise spatial decomposition of the input, for an image of a face this is typically described in terms of pixels which combine into edges, which combine into contours, into simple parts of faces, and finally into entire faces. This is achieved by repeating alternating convolution and pooling operations across stages. At the first stage, in the convolution operation, the image is transformed by a set of several (learned) filters with a limited spatial extent (typically a small sub-region of the image). After which the pooling operation reduces the dimensionality of the convolution. At each subsequent convolution-pooling stage, the output of the previous stage is convolved by another set of (learned) filters and subsequently pooled [4]. As a consequence, both the complexity of the composite transformation and the image area covered increases with each stage [22]. Therefore, relatively simple visual patterns with a small spatial extent are processed at the early stages, whereas more complex visual patterns with a large spatial extent are processed at the later stages [4], [6]. This dependency closely ties the representation and recognition of a visual pattern to its spatial extent, and thus to a specific stage in the network [23], [24].

The strength of this dependency is determined by the network architecture in which the amount of subsampling (e.g., via strided operations or pooling) is specified, this also determines the size of the spatial output of the network. In the case of a simple two layer network with 2×2 filters as in Figure 3, the network produces a single spatial output per 4×4 region in the input. Whereas in a deeper network (containing strided and pooling operations such as in [1]) a single output can describe a 64×64 pixel region of the input. Because the amount of subsampling is determined by the network architecture, the size of the output, or spatial output map, scales with the size of the input. Due to the scaling the relative portion of the input described by a single output node decreases: a 4×4 pixels image can be described with 4 non-overlapping 2×2 filters, where each filter describes one-fourth of the image. Yet for an 8×8 image it would require 16 identically sized filters to cover the input, reducing the portion of the image described by each filter to one-sixteenth. The reduction in relative proportion described by a single output strongly influences the characteristics of the filters in the network. Filters that describe one-sixteenth of a portrait picture might only correspond to a part of a nose, or an ear, whereas filters that cover one-fourth of the picture might correspond to an entire cheek, chin, or forehead. For artist attribution this means that a network with filters that cover relatively small parts of the input are suitable to describe the fine characteristics but cannot describe the composition or iconography of the artwork. As such the network architecture
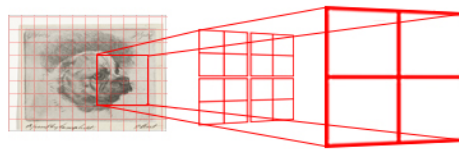

Fig. 3. A 2×2 filter applied to the output of 4 filters of the same size in a lower layer corresponds to a 4×4 region in the input image.

should be chosen in concurrence with the resolution of the input.

Because training CNNs on an image dataset results in a hierarchy of feature representations with increasing spatial extent, a network capable of analysing the entire range from fine to coarse visual characteristics in an image requires many stages in order to capture all the intermediate scales. Moreover, as to not discard information by subsampling between stages, the subsampling has to be performed gradually. Gradual subsampling is performed by having a very deep network with many stages, each subsampling a little. The complexity and the number of parameters in a network is determined by the number of layers and the number of parameters per layer, as such, increasing the number of layers increases the complexity of the network. A more complex network requires more training data, which despite the increasing availability of images of artworks is still lacking. Moreover, the computational demand of the network increases strongly with the complexity of the network, making it infeasible to train a sufficiently complex network [25]. An alternative to increasing the complexity of an individual CNN is to distribute the task over specialised CNNs and combining the resulting predictions into a single one. The biologically motivated multi-column CNN architecture [26] is an example of such an approach.

The multi-scale CNN presented in this paper is based on a multi-scale image representation, whereby a separate CNN is associated with each scale. This allows the scale-specific CNNs to develop both scale-variant and scale-invariant features. The multi-scale representation is created using a Gaussian pyramid [27]. The bottom level of the pyramid corresponds to the input image, subsequent levels contain smoothed (and down-sampled) versions of the previous levels. A visual representation of the model architecture is shown in Figure 4. Note that down-sampling is not necessary to create the higher pyramid levels, and that it is possible to fix the resolution and only change the scale. However, smoothing results in a redundancy between neighbouring pixels, as they convey the same information.

IV. IMAGE CLASSIFICATION TASK

The proposed multi-scale CNN will be evaluated on a task involving a large data set of images of artworks that are heterogeneous in scale and resolution. In our previous work, we have applied a single CNN to a comparable dataset to study computational artist attribution (where the task was to determine who authored a given artwork) [28]. For artist attribution there is often insufficient information on a single
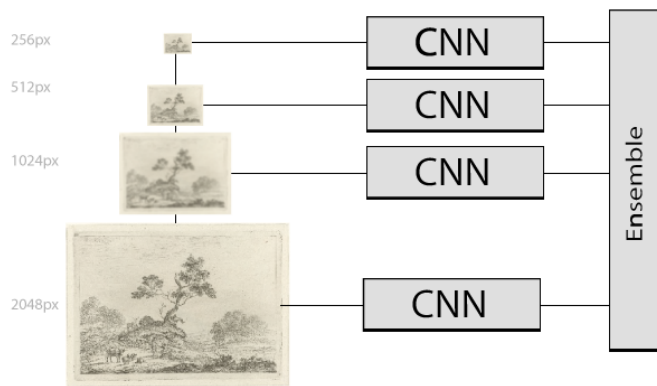
Fig. 4.   Visual representation of the model architecture.

scale to distinguish between very similar artists. For instance, the works of two different artists who use very similar materials to create artworks depicting different scenes might be indistinguishable when considering the very fine details only. Alternatively, when artists create artworks depicting a similar scene using different materials, these may be indistinguishable at a coarse spatial scale. Hence, successful artist attribution requires scale-variant features in addition to scale-invariant features.

Artist attribution is typically performed by combining current knowledge on the artist's practices, technical data, and a visual assessment of the artwork as to establish its origin and value from an economical and historical perspective [29]. In recent years it has been shown that this visual assessment can be performed computationally and can lead to promising results on artist attribution image classification tasks [30], [29], [31], [32], [33], [34]. The increased availability of visual data from the vast digital libraries of museums and the challenges associated with the unique nature of artworks has led to an interest in this domain by researchers from a large diversity of fields. This diversity has resulted in a great many different approaches and techniques aimed at tackling the problem of visual artist attribution. The visual assessment of artworks by art experts generally focuses on textural characteristics of the surface (e.g., the canvas) or on the application method (e.g., brushstrokes) [35], this in turn has shaped many of the computational approaches to visual artwork assessment (e.g., [29], [36], [33]).

More recently it has been shown that general purpose computer vision approaches can be used for the visual assessment of artworks, specifically SIFT features [37] and deep-based representations as learned by a CNN for a general object recognition task (i.e., ImageNet) [38], [39] can be used to perform image classification tasks on artworks. This development is a deviation from the practice as performed by art experts, with the focus shifted from small datasets of a few artists with high resolution images (5 to 10 pixels per mm) to large datasets with many artists and lower resolution images (0.5 to 2 pixels per mm). By using images of a lower resolution the amount of details related to the artist's specific style in

terms of application method (e.g., brushstrokes) and material choices (e.g., type of canvas or paper) become less apparent, which shifts the focus to coarser image structures and shapes. However, using a multi-scale approach to artist attribution it is possible to use information from different scales, learning features appropriate from both coarse and fine details.

V. Experimental setup

This section describes the setup of the artist attribution experiment. The setup consists of a specification of the CNN architecture, the dataset, the evaluation, and the training parameters.

A. multi-scale CNN architecture

The multi-scale CNN architecture used in this work is essentially an ensemble of single-scale CNN, where the single-scale CNN matches the architecture of the previously proven ImageNet model described in [40]. We made two minor modifications to the architecture described in [40] in that we (1) replaced the final 6×6 average pooling layer with a global average pooling layer which averages the final feature map regardless of its spatial size, and (2) reduce the number of ouputs of the softmax layer to 210 to match the number of classes in our dataset. A detailed specification of the single-scale CNN architecture can be found in Table I, where conv-n denotes a convolutional layer with f filters with a size ranging from 11×11 to 1×1. The stride indicates the step size of the convolution in pixels, and the padding indicates how much zero padding is performed before the convolution is applied.

The single-scale CNN architecture used is fully-convolutional, which means that except for the final global average pooling layer it consists solely of convolutional layers. Rather than having max or average pooling layers in the network a convolutional layer with a stride greater than 1 (typically 2) is used. This convolutional layer effectively performs the pooling, but combines it with an additional (learnt) non-linear transformation. A fully convolutional architecture has two main benefits for the work described in this paper: (1) unlike traditional CNN, a fully-convolutional CNN places no restrictions on the input in terms of resolution; the same architecture can be used for varying resolutions, and (2) it can be trained on patches and evaluated on whole images, which makes training more efficient and evaluation more accurate.

Additionally, this architecture has been shown to work well with Guided Backpropagation (GB) [40]. GB is an approach (akin to 'deconvolution' [41]) that makes it possible to visualise what the network has learnt, or which parts of an input image are most characteristic of a certain artist. GB consists of performing a backward pass through the network and computing the gradient w.r.t. an input image. In order to visualise which parts of an image are characteristic of an artist, the activations of the softmax class posterior layer are all set to zero, except the activation for the artist of interest, and subsequently the gradient w.r.t. an input image will activate strongest in the areas characteristic of that artist.

TABLE I
CNN ARCHITECTURE OF SINGLE-SCALE NETWORKS AS USED IN THIS
PAPER. CONVn DENOTE CONVOLUTIONAL LAYERS. DURING TRAINING A
224×224 PIXELS CROP IS USED, THE TESTING IS PERFORMED ON THE
ENTIRE INPUT IMAGE (WHICH SHORTEST SIDE IS IN THE RANGE OF 256 UP
TO 2048 PIXELS).

Layer	Filters	Size, stride, pad	Description
Training Data	-	224×224, -, -	RGB image crop
Testing Data	-	Entire image, -, -	Full RGB image
conv1.1	96	11×11, 4, 0	ReLU
conv1.2	96	1×1, 1, 0	ReLU
conv1.3	96	3×3, 2, 1	ReLU
conv2.1	256	5×5, 1, 2	ReLU
conv2.2	256	1×1, 1, 0	ReLU
conv2.3	256	3×3, 2, 0	ReLU
conv3.1	384	3×3, 1, 1	ReLU
conv3.2	384	1×1, 1, 0	ReLU
conv3.3	384	3×3, 2, 0	ReLU + Dropout (50%)
conv4	1024	1×1, 1, 0	ReLU
conv5	1024	1×1, 1, 0	ReLU
conv6	210	1×1, 1, 0	ReLU
global-pool	-	-	Global average
softmax	-	-	Softmax layer

Fig. 5. Digital photographic reproduction of *'Kop van een koe met touw om de horens'* by Jacobus Cornelis Gaal.

Our multi-scale is constructed as an ensemble, or multi-column [21], architecture, in which the softmax class-posteriors of the single-scale CNN are averaged and used as the final predictions for evaluation, the evaluation procedure is further described in Section V-D.

B. Dataset

The dataset[1] consists of $58,630$ digital photographic reproductions of print artworks by 210 artists retrieved from the collection of the Rijksmuseum, the Netherlands State Museum. These artworks were chosen based on the following four criteria: (1) Only printworks made on paper, (2) by a single artist, (3) public domain, and (4) at least 96 images by the same artist match these criteria. This ensured that there were sufficient images available from each artist to learn to recognise their work, and excluded any artworks which are visually distinctive due to the material choices (e.g., porcelain). An example of a print from the Rijksmuseum collection is shown in Figure 5.

For many types of artworks there is a large degree of variation in their physical size: there are paintings of several meters in width or height, and paintings which are only tens of centimeters in width or height. Moreover, for such artworks there is a large degree of variation in the ratio of pixels per mm and as such the dimension of the reproductions in pixels. Yet, this makes it very appealing to work with print artworks, as they are much more uniform in terms of physical size as for example paintings. While there is still some variation in physical size for print artworks, as shown in Figure 6. Previous approaches have dealt with such variations by resizing all images to a single size, which confounds image resolution with physical resolution.

Normalising the images to obtain fixed pixel to mm ratios would result in a loss of visual detail. Given that our aim

is to have our multi-scale CNN develop both scale-invariant and scale-variant filters, we take the variation in scales and resolutions for granted.

A four-level Gaussian (low-pass) pyramid is created following the standard procedure for creating Gaussian Pyramids described in [27], [42]. Initially all images are resized so that the shortest side (height or width) is 2048 pixels, as to preserve the aspect ratio, creating the first pyramid level. From this first level the subsequent pyramid level is created by smoothing the previous level, and down-sampling by removing every other pixel column and row (effectively reducing the image size by a factor two). This smoothing and down-sampling step is repeated, every time taking the previous level as the starting point, to create the remaining two pyramid levels. The smoothing steps were performed by recursively convolving the images with the Gaussian kernel G, which is defined as:

$$
G = \frac{1}{256}
\begin{bmatrix}
1 & 4 & 6 & 4 & 1 \\
4 & 16 & 24 & 16 & 4 \\
6 & 24 & 36 & 24 & 6 \\
4 & 16 & 24 & 16 & 4 \\
1 & 4 & 6 & 4 & 1
\end{bmatrix}
$$

.

The resulting Gaussian pyramid consists of four levels of images with the shortest side being 256, 512, 1024, and 2048 pixels for each level respectively.

The dataset is divided into a training (70%), validation (10%), and test set (20%). The training set is used to train the network, the validation set is used to optimise the hyperparameters, and the evaluation set is used to estimate the prediction performance. All results reported in this paper are based on the test set.

C. Training parameters

All networks were trained using an effective training procedure (cf. [1]), with the values of the learning rate, momen-

---

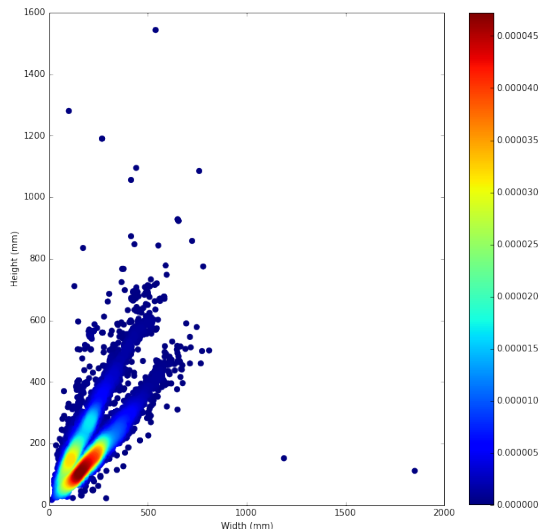[1]The dataset is available at https://auburn.uvt.nl/.

Fig. 6. Scatter plot of physical dimensions of the artworks in the test set in millimeters; each point represents an artwork, its colour indicating the density in the area around it. The scatter plot shows that there are two predominant shapes of artworks: square artworks and rectangular artworks (width slightly greater than height). The majority of the artworks cluster around a size of 250×250 mm.

tum, and weight decay hyperparameters being 10^{-2}, 0.9, and $5 \cdot 10^{-4}$ respectively. Whenever the error on the validation set stopped decreasing the learning rate was decreased by a factor 10.

D. Evaluation

The evaluation is performed on entire images. The fully-convolutional nature of the multi-scale CNN makes it unnecessary to perform cropping. The scale-specific prediction for an image is the average over the spatial output map, resulting in a single scale-specific prediction for the entire image. The performance on all experiments is reported using the Mean Class Accuracy (MCA), which is the average of the accuracy scores obtained per artist. We report the MCA because it is not sensitive to unbalanced classes and it allows for a comparison of the results with those reported in [37], [28]. The MCA is equal to the mean of the per class precision, as such we also report the mean of the per class recall, and the harmonic mean of these mean precision and mean recall measures, also known as the F-score.

Additionally, we compare our results to those obtained by performing multi-scale training as described in [20]. We implemented multi-scale training using the same CNN architecture as used previously, and only varied the input data. Rather than blurring the images before subsampling the images, we follow [20] and directly subsample the images, as such the scales do not form a Gaussian Pyramid. Because the highest scale is not blurred in either case these results are identical, and are produced by the same network.

Furthermore, we report the pair-wise correlations between the Class Accuracy (CA) for each artist for the four different scales for both approaches. The pair-wise correlations between

TABLE II
MEAN CLASS ACCURACIES, MEAN RECALL AND F-SCORE FOR THE FOUR INDIVIDUAL SCALES AND THE ENSEMBLE OF FOUR SCALES FOR OUR APPROACH.

Scale	MCA	Mean recall	F-Score
256	70.36	65.03	67.59
512	75.69	69.70	72.57
1024	67.69	44.08	53.48
2048	62.03	38.54	47.55
Ensemble	**82.11**	**72.50**	**77.01**

TABLE III
MEAN CLASS ACCURACIES FOR ALL POSSIBLE SCALE COMBINATIONS OBTAINED WITH OUR APPROACH, A '+' INDICATES INCLUSION OF THE SCALE. IN BOLD ARE THE COMBINATIONS WHICH LEAD TO THE BEST COMBINED PERFORMANCE IN EACH BLOCK. THE BEST OVERALL SCORE IS UNDERLINED.

256	512	1024	2048	MCA	Mean recall	F-Score
+				70.36	65.03	67.59
	+			**75.69**	**69.7**	**72.57**
		+		67.96	44.08	53.48
			+	62.03	38.54	47.55
+	+			78.06	**71.61**	**74.69**
+		+		75.92	67.65	71.54
+			+	76.24	67.92	71.84
	+	+		79.15	67.71	72.98
	+		+	**80.21**	68.11	73.66
		+	+	71.41	45.4	55.51
+	+	+		80.15	72.14	75.94
+	+		+	80.87	**72.47**	**76.44**
+		+	+	79.27	68.89	73.72
	+	+	+	**80.95**	65.9	72.66
+	+	+	+	82.12	72.5	77.01

TABLE IV
MEAN CLASS ACCURACIES, MEAN RECALL AND F-SCORE FOR THE FOUR INDIVIDUAL SCALES AND THE ENSEMBLE OF FOUR SCALES USING MULTI-SCALE TRAINING [20].

Scale	MCA	Mean recall	F-Score
256	70.56	65.74	68.07
512	73.5	68.36	70.84
1024	65.63	57.96	61.56
2048	62.03	38.54	47.55
Ensemble	**79.98**	**73.02**	**76.34**

scales indicates the similarity of the performance for individual artists at those two scales. A high correlation indicates that the attributions of an artist are largely the same at both scales, whereas a low correlation indicates that the artworks of an artists are classified differently at the two scales which suggests the relevance of scale-specific information.

VI. RESULTS

The results of each individual scale-specific CNN of the multi-scale CNN and the ensemble averages are reported in Table II. The best-performing single scale is 512. The ensemble-averaged score of the multi-scale CNN outperforms each individual scale by far. As is evident from Table III, no combination of three or fewer scales outperforms the multi-scale (four-scale) CNN. We report the results obtained by multi-scale training [20] in Table IV. The results of all possible combinations of these results are reported in Appendix A.

The MCA and mean recall obtained for the resolutions

	256	512	1024	2048
256	1.00	0.56	0.27	0.18
512	0.56	1.00	0.44	0.29
1024	0.27	0.44	1.00	0.54
2048	0.18	0.29	0.54	1.00

	256	512	1024	2048
256	1.00	0.60	0.33	0.26
512	0.60	1.00	0.52	0.35
1024	0.33	0.52	1.00	0.40
2048	0.26	0.35	0.40	1.00

Top five artists with least variation between scales.				
Artist	256	512	1024	2048
Johannes Janson	66.67	65.12	67.74	65.22
Pieter de Mare	80.0	82.67	86.0	81.25
Jacobus Ludovicus Cornet	73.53	76.47	73.33	79.17
Cornelis van Dalen (II)	100.0	94.44	100.0	100.0
Lucas Vorsterman (I)	85.42	89.8	83.67	88.57
Top five artists with most variation between scales.				
Artist	256	512	1024	2048
Joannes van Doetechum (I)	100.0	100.0	0.0	0.0
Totoya Hokkei	100.0	0.0	0.0	0.0
Gerrit Groenewegen	88.89	100.0	100.0	0.0
Abraham Genoels	86.67	64.29	0.0	0.0
Charles Meryon	64.0	86.67	100.0	0.0

greater than 512 decrease, this suggests that there is a ceiling in performance and that further increasing the resolution would not help to improve the performance. Yet, combining the predictions from each scale in an ensemble results in a boost in performance. The pair-wise correlations between scales as reported in Table V show larger correlations for adjacent scales than for non-adjacent scales. This pattern of correlations agrees with the causal connection of adjacent scales. Additionally, we also report the correlations between the scales using multi-scale training (c.f. [20]) in Table VI. We note that in general the correlations in the latter case are stronger than the former, which shows that there is a greater performance difference across artists between scales for our approach, which indicates that the single-scale CNN for our approach learn a greater variety of scale-variant features.

To provide some insight on artist-specific relevance of the four different scales, Table VII lists the top five artists with the least and most variation between scales as determined by the standard deviation of their MCA across scales. From this table it can be observed that there is a large variation between artists in terms of which scales work well, where for some artists performance is highly scale-specific (a perfect performance is achieved on one scale and a completely flawed performance on another), and for others performance does not depend on scale (the performance is stable across scales).

To illustrate the effect of resolution on the automatic detection of artist-specific features, Guided Backpropagation [40] was used to create visualisations of the artwork *'Hoefsmid bij een ezel'* by Jan de Visscher at the four scales. Figure 7 shows the results of applying Guided Backpropagation to the art work. The visualisations show the areas in the input image that the network considers characteristic of Jan de Visscher for that scale. A clear shift to finer details is observed when moving to higher resolutions.

As the multi-scale CNN produces a prediction vector for each image we are able to calculate the similarity of the artworks in terms of the distance in a high-dimensional space. Using t-SNE [43] we visualise these distances in a two-dimensional space in Figure 8, the spatial distance indicates the similarity between images at determined by the ensemble. The t-SNE visualisation of the distances shows a clear clustering of similar artworks, in terms of shape, colour, and content.

From these visualisations we can observe that the multi-scale representation is able to express the similarities between artworks in terms of both fine and coarse characteristics. Moreover, multi-scale representation makes it possible to express the similarity between artworks which are only similar on some scales (i.e., if only the fine, or only the coarse characteristics are similar), as shown in Figure 8.

VII. DISCUSSION

In this work we explored the effect of incorporating scale-variance, as put forward by Gluckman [9], in CNN and how it can be used to learn deep image representations that deal well with variations in image resolution, object size, and image scale. The main idea behind scale-variance is that decomposing an image in scale-invariant components results in an incomplete representation of the image, as a part of the image structure is not scale-invariant. As stated in Section I Gluckman showed that image classification performance can be improved by using the scale variant image structure. This means that a good multi-scale image representations is capable of capturing both the task-relevant scale-variant and scale-invariant image structure. To this end we presented an approach for learning scale-variant and scale-invariant representations by means of an ensemble of scale-specific CNN. By allowing each scale-specific CNN to learn the features which are relevant for the task at that scale, regardless whether they are scale-invariant or not, we are able to construct a multi-scale representation that captures both scale-variant and scale-invariant image features.

We demonstrated the effectiveness of our multi-scale CNN approach on an artist attribution task, on which it outperformed a single-scale CNN and was superior to the state-of-the-art performance on the attribution task. Furthermore, we show that the best performance is achieved by combining all scales, exploiting the fact that scale-specific attribution performance varies greatly for different artists.

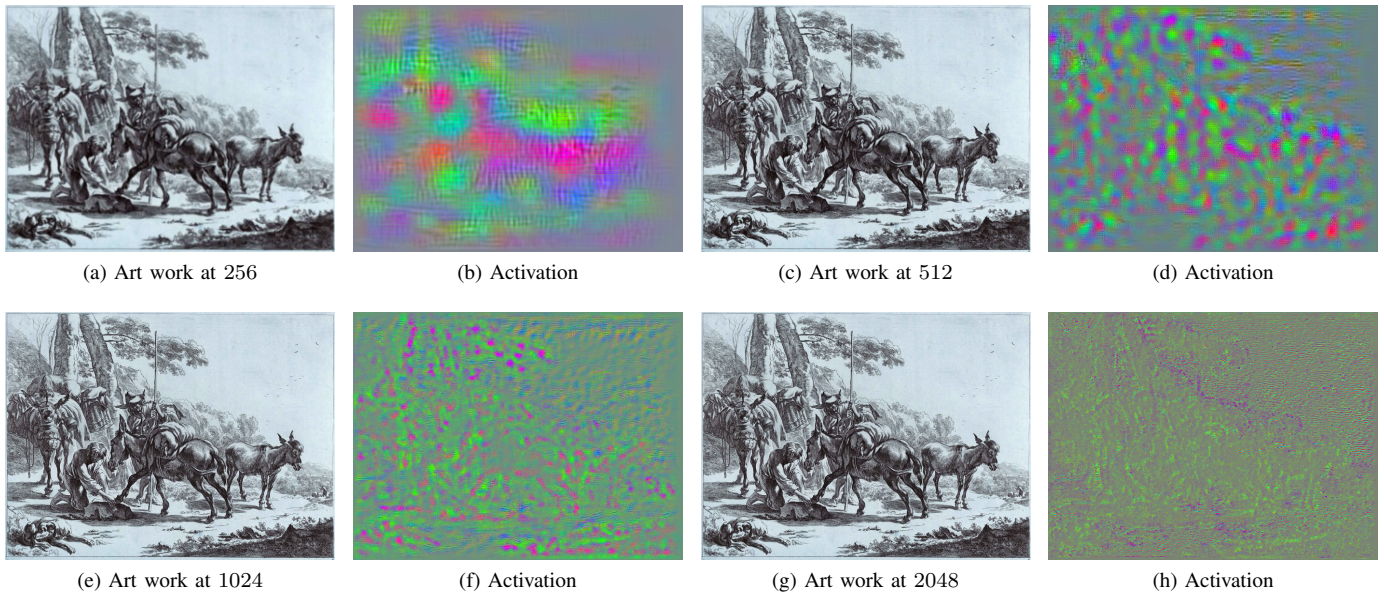Is a multi-scale approach really necessary? Our approach requires multiple scale-specific CNNs, which may be com-

(a) Art work at 256   (b) Activation   (c) Art work at 512   (d) Activation

(e) Art work at 1024   (f) Activation   (g) Art work at 2048   (h) Activation

Fig. 7. Visualisations of the activations for the artwork *'Hoefsmid bij een ezel'* by Jan de Visscher at four scales. The activation shows the importance of the highlighted regions for correctly identifying the artist, the colours have been contrast enhanced for increased visibility. Best viewed in colour.
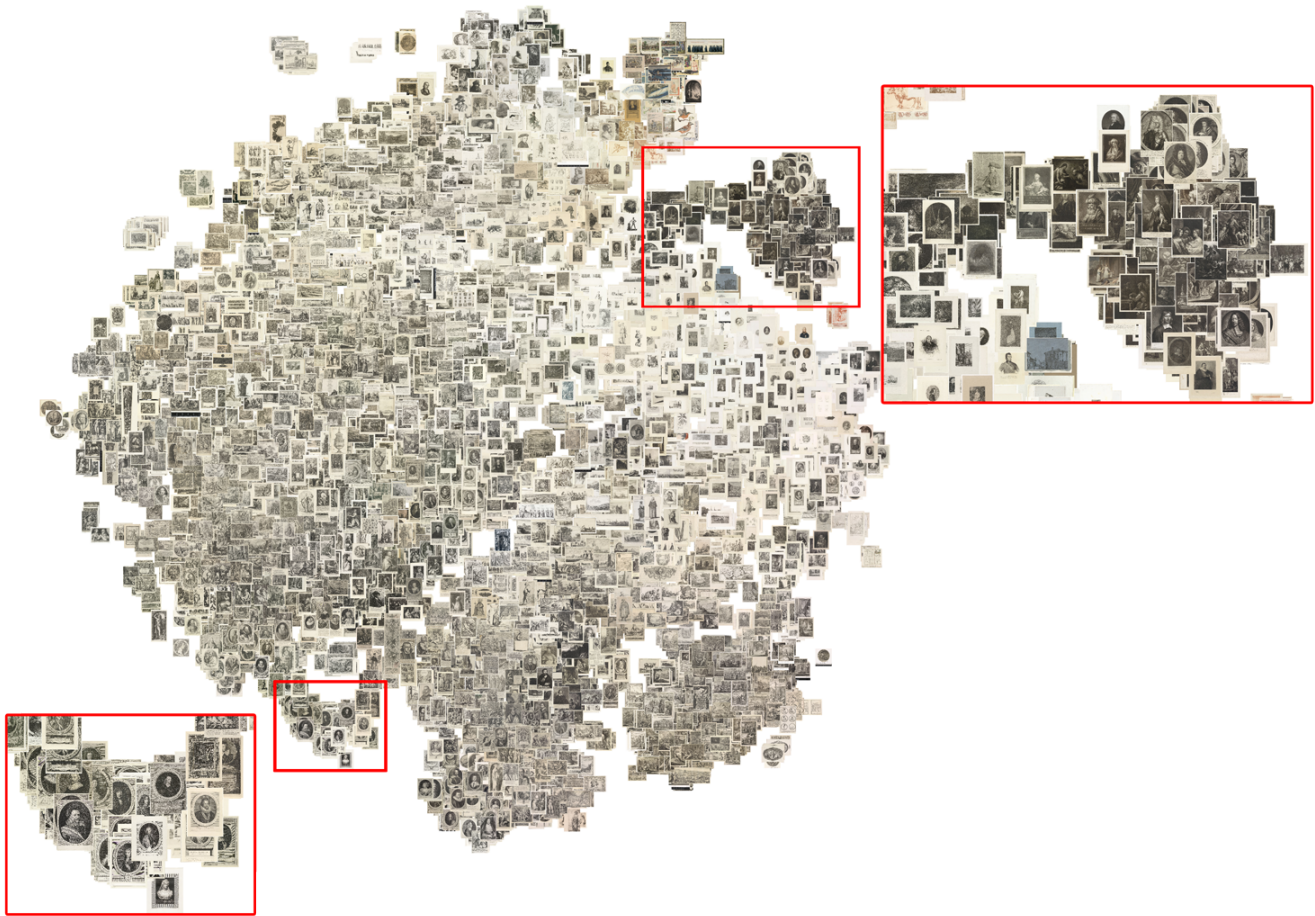

Fig. 8. t-SNE plot of all artworks in the test set where spatial distance indicates the similarity as observed by the network. Zoomed excerpts shown of outlined areas, illustrating examples of highly similar clusters.

bined into a single more sophisticated CNN which acquires coarse- to fine-grained features, using high resolution images. However, such a network would have to be significantly deeper and more complex than the network used in this paper. Which would increase the computational cost for training and the amount of training data that is needed beyond what is practically feasible at this time. Therefore, we cannot rule out that a single sophisticated CNN may obtain a similar performance as our multi-scale CNN. Moreover, we suspect that such a network will struggle with coarse characteristics which are very dissimilar when observed at a fine scale, but very similar on a coarse scale, as the coarse scale analysis is conditioned on the fine scale analysis. Therefore, we expect that a single very complex CNN will not work as well as our multi-scale CNN.

Additionally, we compared our approach to Multi-scale training [20] and showed that construction a Gaussian Pyramid of the input increases performance and decreases the correlations between scales. While constructing the Gaussian Pyramid increases the computational load slightly, we believe that the reduced correlations between scales implies that our approach is better at capturing the scale variant characteristics, and is subsequently able to leverage these for increased performance.

Compared to previously proposed CNN architectures that deal with scale-variation, our approach requires many more model parameters, as the parameters are not shared between the single-scale CNN. However, we consider this a key attribute of the approach as it enables the model to learn scale-variant features, and moreover, because the parameters are not shared the models can be trained independently and in parallel. Despite this, a potential downside of our approach is that we do not explicitly learn scale-invariant features, while they might implicitly emerge from the training procedure, future work on how to explicitly learn scale-variant and scale-invariant features is needed.

We expect that the use of multi-scale CNNs will improve performances on image recognition tasks that involve images with both fine and coarse-grained task-relevant details. Examples of such tasks are scene classification, aerial image analysis, and biomedical image analysis.

VIII. Conclusion

There is a vast amount visual information to be gleaned from multi-scale images in which both the coarse and the fine grained details are represented. However, capturing all of this visual information in a deep image representation is non trivial. In this paper we proposed an approach for learning scale-variant and scale-invariant representations from high-resolution images. By means of a multi-scale CNN architecture consisting of multiple single-scale CNN, we exploit the strength of CNN in learning scale-variant representations, and combine these over multiple scales to encourage scale-invariance and improve performance. We demonstrate this by analysing the large amount of available details in multi-scale images for a computational artist attribution task, improving on the current state-of-the-art.

Moreover, we found that the representations at the various scales differ both in performance and in image structure learnt, and that they are complementary: averaging the class posteriors across all scales leads to optimal performance. We conclude by stating that encouraging the combined development of scale-invariant and scale-variant representations in CNNs is beneficial to image recognition performance for tasks involving image structure at varying scales and resolutions and merits further exploration.

References

[1] A. Krizhevsky, I. Sutskever, G. Hinton, ImageNet Classification with Deep Convolutional Neural Networks., in: Advances in Neural Information Processing Systems 25, 2012, pp. 1097–1105.

[2] K. He, X. Zhang, S. Ren, J. Sun, Deep Residual Learning for Image Recognition, ArXiv arXiv:1512.03385.

[3] Y. Gong, L. Wang, R. Guo, S. Lazebnik, Multi-scale Orderless Pooling of Deep Convolutional Activation Features, ArXiv (2014) 1–17 arXiv:1403.1840.

[4] Y. LeCun, Y. Bengio, Convolutional networks for images, speech, and time series, The handbook of brain theory and neural networks 3361 (1995) 255–258. doi:10.1109/IJCNN.2004.1381049.

[5] S. R. Kheradpisheh, M. Ghodrati, M. Ganjtabesh, T. Masquelier, Deep Networks Resemble Human Feed-forward Vision in Invariant Object Recognition, ArXiv arXiv:1508.03929.

[6] Y. Xu, T. Xiao, J. Zhang, K. Yang, Z. Zhang, Scale-Invariant Convolutional Neural Networks, ArXiv arXiv:1411.6369.

[7] R. C. Gonzalez, R. E. Woods, Digital Image Processing (3rd Edition), Prentice-Hall, Inc., Upper Saddle River, NJ, USA, 2006.

[8] T. Lindeberg, Scale-space theory: a basic tool for analyzing structures at different scales, Journal of Applied Statistics 21 (1) (1994) 225–270. doi:10.1080/757582976.

[9] J. Gluckman, Scale variant image pyramids, in: Computer Vision and Pattern Recognition, 2006, 2006. doi:10.1109/CVPR.2006.265.

[10] C. Park, Dennis and Ramanan, Deva and Fowlkes, Multiresolution models for object detection, in: ECCV 2010, 2010, pp. 1–14.

[11] D. G. Lowe, Distinctive image features from scale invariant keypoints, Int'l Journal of Computer Vision 60 (2).

[12] K. Lenc, A. Vedaldi, Understanding image representations by measuring their equivariance and equivalence, Computer Vision and Pattern Recognition (CVPR), 2015 IEEE Conference on (2015) 991–999.

[13] Q. Le, J. Ngiam, Z. Chen, D. H. Chia, P. Koh, Tiled convolutional neural networks., Nips (2010) 1–9.

[14] P. Sermanet, D. Eigen, X. Zhang, M. Mathieu, R. Fergus, Y. LeCun, OverFeat: Integrated Recognition, Localization and Detection using Convolutional Networks arXiv:1312.6229.

[15] A. Kanazawa, A. Sharma, D. Jacobs, Locally Scale-Invariant Convolutional Neural Networks, in: NIPS, 2014, pp. 1–11. arXiv:1412.5104.

[16] M. Jaderberg, K. Simonyan, A. Zisserman, K. Kavukcuoglu, Spatial Transformer Networks, Nips'15 (2015) 1–14 arXiv:1506.02025.

[17] C. Szegedy, W. Liu, Y. Jia, P. Sermanet, S. Reed, D. Anguelov, D. Erhan, V. Vanhoucke, A. Rabinovich, Going Deeper with Convolutions, arXiv (2014) 1–12 arXiv:1409.4842.

[18] K. Simonyan, A. Zisserman, Very Deep Convolutional Networks for Large-Scale Image Recognition, ArXiv (2015) 1–14 arXiv:1409.1556.

[19] R. Girshick, Fast R-CNN, Arxiv arXiv:1504.08083, doi:10.1109/ICCV.2015.169.

[20] R. Wu, S. Yan, Y. Shan, Q. Dang, G. Sun, Deep Image: Scaling up Image Recognition, Arxiv (2015) 12 arXiv:1501.02876.

[21] D. Cirean, U. Meier, J. Schmidhuber, Multi-column Deep Neural Networks for Image Classification, International Conference of Pattern Recognition (February) (2012) 3642–3649.

[22] C. Garcia, M. Delakis, Convolutional face finder: A neural architecture for fast and robust face detection, IEEE Transactions on Pattern Analysis and Machine Intelligence 26 (11) (2004) 1408–1423.

[23] P. Sermanet, Y. Lecun, Traffic sign recognition with multi-scale convolutional networks, Proceedings of the International Joint Conference on Neural Networks (SEPTEMBER 2011) (2011) 2809–2813.

[24] B. Hariharan, P. Arbeláez, R. Girshick, J. Malik, Hypercolumns for Object Segmentation and Fine-grained Localization, ArXiv arXiv:1411.5752.

[25] L. Hou, D. Samaras, T. Kurc, Y. Gao, Efficient Multiple Instance Convolutional Neural Networks for Gigapixel Resolution Image Classification, arXiv arXiv:1504.07947.

[26] D. Cirean, U. Meier, J. Masci, J. Schmidhuber, Multi-column deep neural network for traffic sign classification, Neural Networks 32 (2012) 333–338. arXiv:arXiv:1202.2745v1, doi:10.1016/j.neunet.2012.02.023.

[27] E. H. Adelson, C. H. Anderson, J. Bergen, P. Burt, J. M. Ogden, Pyramid methods in image processing, RCA Engineer 29 (6) (1984) 33–41. doi:10.1.1.59.9419.

[28] N. van Noord, E. Hendriks, E. Postma, Towards discovery of the artist's style: Learning to recognise artists by their artworks, IEEE Signal Processing Magazine (2015) 1–8.

Appendix

TABLE I
MEAN CLASS ACCURACIES FOR ALL POSSIBLE SCALE COMBINATIONS USING THE MEAN-SCALE TRAINING PROCEDURE DESCRIBED IN [20], A '+' INDICATES INCLUSION OF THE SCALE. IN BOLD ARE THE COMBINATIONS WHICH LEAD TO THE BEST COMBINED PERFORMANCE IN EACH BLOCK. THE BEST OVERALL SCORE IS UNDERLINED.

256	512	1024	2048	MCA	Mean recall	F-Score
+				70.56	65.74	68.07
	+			**73.5**	**68.36**	**70.84**
		+		65.63	57.96	61.56
			+	62.03	38.54	47.55
+	+			75.93	**71.02**	**73.4**
+		+		75.13	70.2	72.58
+			+	75.68	68.08	71.68
	+	+		74.8	68.51	71.51
	+		+	**77.8**	66.2	71.53
		+	+	68.7	54.69	60.9
+	+	+		78.21	**72.94**	**75.48**
+	+		+	**79.16**	71.95	75.38
+		+	+	77.72	70.54	73.95
	+	+	+	77.04	66.65	71.47
+	+	+	+	**79.98**	**73.02**	**76.34**

[29] C. R. Johnson, Jr., E. Hendriks, I. J. Berezhnoy, E. Brevdo, S. M. Hughes, I. Daubechies, J. Li, E. Postma, J. Z. Wang, Image processing for artist identification, IEEE Signal Processing Magazine (Special Section - Signal Processing in Visual Cultural Heritage) (25) (2008) 37–48.

[30] R. Taylor, R. Guzman, T. Martin, Authenticating Pollock paintings using fractal geometry, Pattern Recognition Letters 28 (6) (2007) 695–702.

[31] J. M. Hughes, D. J. Graham, D. N. Rockmore, Quantification of artistic style through sparse coding analysis in the drawings of Pieter Bruegel the Elder., Proceedings of the National Academy of Sciences of the United States of America 107 (4) (2010) 1279–1283. doi:10.1073/pnas.0910530107.

[32] L. J. P. van der Maaten, E. O. Postma, Texton-Based Analysis of Paintings, in: SPIE Optical Imaging and Applications, Vol. 7798, 2010.

[33] J. Li, L. Yao, E. Hendriks, J. Z. Wang, Rhythmic brushstrokes distinguish van Gogh from his contemporaries: findings via automated brushstroke extraction., IEEE transactions on pattern analysis and machine intelligence 34 (6) (2012) 1159–1176. doi:10.1109/TPAMI.2011.203.

[34] P. Abry, H. Wendt, S. Jaffard, When Van Gogh meets Mandelbrot: Multifractal classification of painting's texture, Signal Processing 93 (3) (2013) 554–572. doi:10.1016/j.sigpro.2012.01.016.

[35] E. Hendriks, S. Hughes, Van Gogh ' s brushstrokes : marks of authenticity ?, Art, Conservation, and Authenticities: Material, Concept, Context (2008) 57–62.

[36] D. H. Johnson, E. Hendriks, C. R. J. Jr, Interpreting canvas weave matches, Art Matters (2012) 53–61.

[37] T. Mensink, J. V. Gemert, The Rijksmuseum Challenge: Museum-Centered Visual Recognition, Proceedings of International Conference on Multimedia Retrieval (2014) 2–5.

[38] S. Karayev, M. Trentacoste, H. Han, A. Agarwala, T. Darrell, A. Hertzmann, H. Winnemoeller, Recognizing Image Style, ArXiv arXiv:1311.3715.

[39] B. Saleh, A. Elgammal, Large-scale Classification of Fine-Art Paintings: Learning The Right Metric on The Right Feature, arXiv (2015) 21 arXiv:1505.00855.

[40] J. T. Springenberg, A. Dosovitskiy, T. Brox, M. Riedmiller, Striving for Simplicity: The All Convolutional Net, in: ICLR, 2015. arXiv:1412.6806.

[41] M. Zeiler, R. Fergus, Visualizing and understanding convolutional networks, ECCV 2014 8689 (2014) 818–833. doi:10.1007/978-3-319-10590-1.

[42] M. Ogden, H. Adelson, R. Bergen, J. Burt, Pyramid-based computer graphics, RCA Engineer.

[43] L. van der Maaten, G. Hinton, Visualizing Data using t-SNE., Journal of Machine Learning Research 9 (2008) 2579–2605.